

- [22] Hewett TE, Myer GD, Ford KR. Decrease in neuromuscular control about the knee with maturation in female athletes. *J Bone Joint Surg Am* 2004;86-A:1601–8.
- [23] Noyes FR, Barber-Westin SD, Heckenstein C, Walsh C, West J. The drop-jump screening test: difference in lower limb control by gender and effect of neuromuscular training in female athletes. *Am J Sports Med* 2005;33:197–207.
- [24] Barber-Westin SD, Galloway M, Noyes FR, Corbett G, Walsh C. Assessment of lower limb neuromuscular control in prepubescent athletes. *Am J Sports Med* 2005;33:1853–60.
- [25] Beynnon BD, Fleming BC, Johnson RJ, Nichols CE, Renstrom PA, Pope MH. Anterior cruciate ligament strain behavior during rehabilitation exercises in vivo. *Am J Sports Med* 1995;23:24–34.
- [26] Renstrom P, Arms SW, Stanwyck TS, Johnson RJ, Pope MH. Strain within the anterior cruciate ligament during hamstring and quadriceps activity. *Am J Sports Med* 1986;14:83–7.
- [27] Krosshaug T, Nakamae A, Boden BP, Engebretsen L, Smith G, Slauterbeck JR, et al. Mechanisms of anterior cruciate ligament injury in basketball: video analysis of 39 cases. *Am J Sports Med* 2007;35:359–67.
- [28] Barber-Westin SD, Noyes FR, Galloway M. Jump-land characteristics and muscle strength development in young athletes: a gender comparison of 1140 athletes 9 to 17 years of age. *Am J Sports Med* 2006;34:375–84.
- [29] Quatman CE, Ford KR, Myer GD, Hewett TE. Maturation engenders gender differences in landing force and vertical jump performance: a longitudinal study. *Am J Sports Med* 2006;34:806–13.

Original article

The effect of geometry of the tibial polyethylene insert on the tibiofemoral contact kinematics in Advance Medial Pivot total knee arthroplasty

GO OMORI¹, NAOAKI ONDA², MASASHI SHIMURA³, TOYOHICO HAYASHI³, TAKASHI SATO⁴, and YOSHIO KOGA⁴

¹Center for Transdisciplinary Research, Niigata University, 2-8050 Igarashi, Nishi-ku, Niigata 950-2181, Japan

²Division of Orthopedic Surgery, Department of Regenerative and Transplant Medicine, Niigata University Graduate School of Medical and Dental Science, Niigata, Japan

³Faculty of Engineering, Niigata University, Niigata, Japan

⁴Orthopedic Surgery, Niigata Kobari Hospital, Niigata, Japan

Abstract

Background. In modern total knee arthroplasty (TKA), it is important to reproduce both medial pivot motion and posterior femoral rollback to obtain greater postoperative knee flexion. Several studies have reported the factors affecting knee motion and range of motion after TKA. The purpose of this study was to evaluate the effect of the tibial insert geometry on the tibiofemoral contact kinematics, especially focusing on the medial pivot motion and posterior femoral rollback.

Methods. Seven cadaveric knees were replaced with the Advance Medial Pivot TKA, and two different geometries of polyethylene tibial insert, the standard medial pivot design (MP-design) and double high design (DH-design), were biomechanically compared. Four experimental configurations were evaluated in each specimen in this order: (1) the MP-design with posterior cruciate ligament (PCL) retaining, (2) the DH-design with PCL retaining, (3) the MP-design with PCL sacrificing, and (4) the DH-design with PCL sacrificing.

Results. Under the PCL-retaining condition, both designs showed no medial pivot but bicondylar femoral rollback more than 60° of knee flexion. In the MP-design, tibiofemoral contact point (estimated contact point, ECP) of the medial compartment was located on the posterior lip of the ball-in-socket structure while demonstrating greater than 120° of knee flexion. The posterior translation was also the same in both designs. On the other hand, ECP of the MP-design and the DH-design showed only medial pivot pattern under the PCL-sacrificing condition. In the DH-design, ECP of the lateral compartment showed paradoxical anterior translation from 0° to 60° of knee flexion. Total posterior translation was significantly greater in the lateral compartment than that in the medial compartment.

Conclusions. The results of this study suggest that in this type of TKA system the ball-in-socket geometry in the MP-design has an advantage for reproducing medial pivot motion in the PCL-sacrificing condition, and the flexion path structure in the

DH-design is considered to be both effective and safe for femoral rollback in the PCL-retaining condition. However, neither design is sufficient to reproduce medial pivot motion and posterior femoral rollback. Therefore, a different design of tibial insert is needed for more physiological kinematics after TKA.

Introduction

An important aim of total knee arthroplasty (TKA) is to return the arthritic knee to as close to normal function as possible. The physiological motion of the knee joint has both medial pivot motion and femoral rollback.^{1–3} This motion pattern is seen not only in the midflexion area but also in a deep flexion range of more than 100°. Therefore, the combination of a medial pivot motion and femoral rollback is thought to be the key motion for high flexion of the knee joint. There are several factors that influence the three-dimensional knee motion after TKA: these include the geometry of the femoral and tibial component, the setting alignment of these implants to the bone, changes in the level of the joint line, soft tissue balance and tension, and retention or sacrifice of the posterior cruciate ligament (PCL).^{5–8} Fluoroscopic studies of modern TKA have not yet demonstrated expected knee motion close to normal conditions but rather a nonphysiological motion such as paradoxical sliding forward or paradoxical rolling forward.^{8–10} Furthermore, these studies have analyzed the knee motion during normal gait, up/down stairs, and rising from/sitting in a chair. In these activities, the maximum flexion of the knee joint is never greater than 90°; therefore, precisely how the knee joint moves after TKA thus remains unclear, especially in deep flexion.

Recently, an asymmetrical tibial polyethylene insert, a ball-in-socket on the medial side and an arcuate

Offprint requests to: G. Omori

Received: February 24, 2009 / Accepted: August 11, 2009

groove on the lateral side, was introduced to reproduce the medial pivot motion during knee extension-flexion.¹¹ In this type of TKA system, the typical medial pivot motion was observed by an *in vivo* kinematic study using fluoroscopy.¹² However, it is not clearly demonstrated whether we should preserve or sacrifice the PCL at surgery. Furthermore, it is unknown whether posterior femoral rollback is reproduced in this type of TKA system. The purpose of the current study was to evaluate the effect of polyethylene tibial insert geometry in the medial pivot TKA on the tibiofemoral contact kinematics in relationship to retaining or sacrificing PCL, especially focusing on the medial pivot motion and posterior femoral rollback in deep knee flexion.

Materials and methods

Seven fresh-frozen cadaveric knee joints were used in this study. Consent for the design of this study was obtained from the Institutional Review Board and the ethical committee of our institute. X-ray examination was previously performed to select knee joints of almost the same size. None of the knees had any evidence of skeletal deformity, and it was confirmed that the PCL was in an intact condition.

After the skin and subcutaneous tissue were stripped, leaving the capsule, ligaments, and muscles intact, each knee was replaced with the Advance Medial Pivot Prosthesis (Wright Medical Technology, Arlington, TN, USA). The distal femur was cut in 5° of valgus and 3° of external rotation. The proximal tibia was cut at a right angle to the tibial axis in the coronal plane and 3° of posterior slope in the sagittal plane. The PCL was preserved, and the patella was not resurfaced. After bone cutting was completed, a size 2 femoral and tibial component with a 10-mm-thick polyethylene insert was placed. The metal rods were inserted into the intramedullary space of the femur and tibia, and the femoral rod was rigidly fixed to the motion frame. The tibial rod was fixed to the clamp that allows 6-degrees-of-freedom motion. The knee joint was moved from 0° to 150° of flexion by a load cell under the loading condition of 40 N on the quadriceps tendon and 20 N on each medial and lateral hamstring muscle through the semitendinosus and biceps femoris tendon. The load ratio of quadriceps and hamstring was according to previous reports; however, the actual amount of load was less than that of the physiological condition as a result of the strength of the motion frame and load cell.^{13,14}

The tibiofemoral contact kinematics was then evaluated using the photostereometric knee motion analysis system (KKN/1B), which was basically developed at our institute (Faculty Engineering, Niigata University). This system consists of eight LEDs (BR 3371X; Stanley

Denshi, Tokyo, Japan) with marker devices mounted onto the femoral and tibial bone, two sets of three linear high resolution CCD cameras (TCD141C; Toshiba, Tokyo, Japan) for tracking the LED position, and a PC for data analysis. The spatial resolution was designed to be 0.06 mm when the LEDs were located on the focal plane of the CCD cameras, and overall accuracy of the measuring system was within 0.52 and 0.11 mm at any point on the femoral component. Three-dimensional computer-aided design (CAD) solid models of the femoral component, tibial tray, and polyethylene insert were obtained, and the positional relationship between these models was also measured. Intersurface distance between the femoral component and polyethylene insert was quantitatively assessed, and the area where the value of the intersurface distance was less than or equal to 0.75 mm was defined as the estimated contact area. The center of the estimated contact area was finally defined as the estimated contact point (ECP), and the contact kinematics was evaluated by changing the ECP.¹⁵⁻¹⁷

In the current study, two different designs of the polyethylene tibial insert were compared: one was the standard medial pivot design (MP-design) and the other was the double high design (DH-design). In the MP-design, a medial socket exactly conformed to the sphere of the femoral component, thus providing the medial ball-in-socket kinematics, and the lateral part was an arcuate groove centered on the medial socket. The basic geometry of the DH design was the same as the MP-design: the main difference between the MP-design and the DH-design was the geometry of the posterior lip. In the MP-design, the geometry of the posterior lip was part of the ball-in-socket and arcuate groove design; on the other hand, the posterior lip of the DH-design was 3 mm lower than that of the MP-design, which resulted in a posterior slope (Fig. 1a-c). The concept of posterior slope was that this slope will act as a "flexion path" when femoral rollback occurs. The medial pivot femoral component was used for both the MP-design and the DH-design. Both medial and lateral condyles of the medial pivot femoral component had a sphere and C-curve design with a single radius in all three planes. Both types of polyethylene inserts were exchanged on the same metal tibial component, so that the difference of the design was directly comparable using the same cadaveric knee joint.

Four experimental configurations were evaluated in each specimen in this order: (1) the MP-design with PCL retaining, (2) the DH-design with PCL retaining, (3) the MP-design with PCL sacrificing, and (4) the DH-design with PCL sacrificing.

At the time of measurement under the PCL-sacrificing condition, the extension gap and the flexion gap were evaluated and a polyethylene insert 2 mm thicker was used.

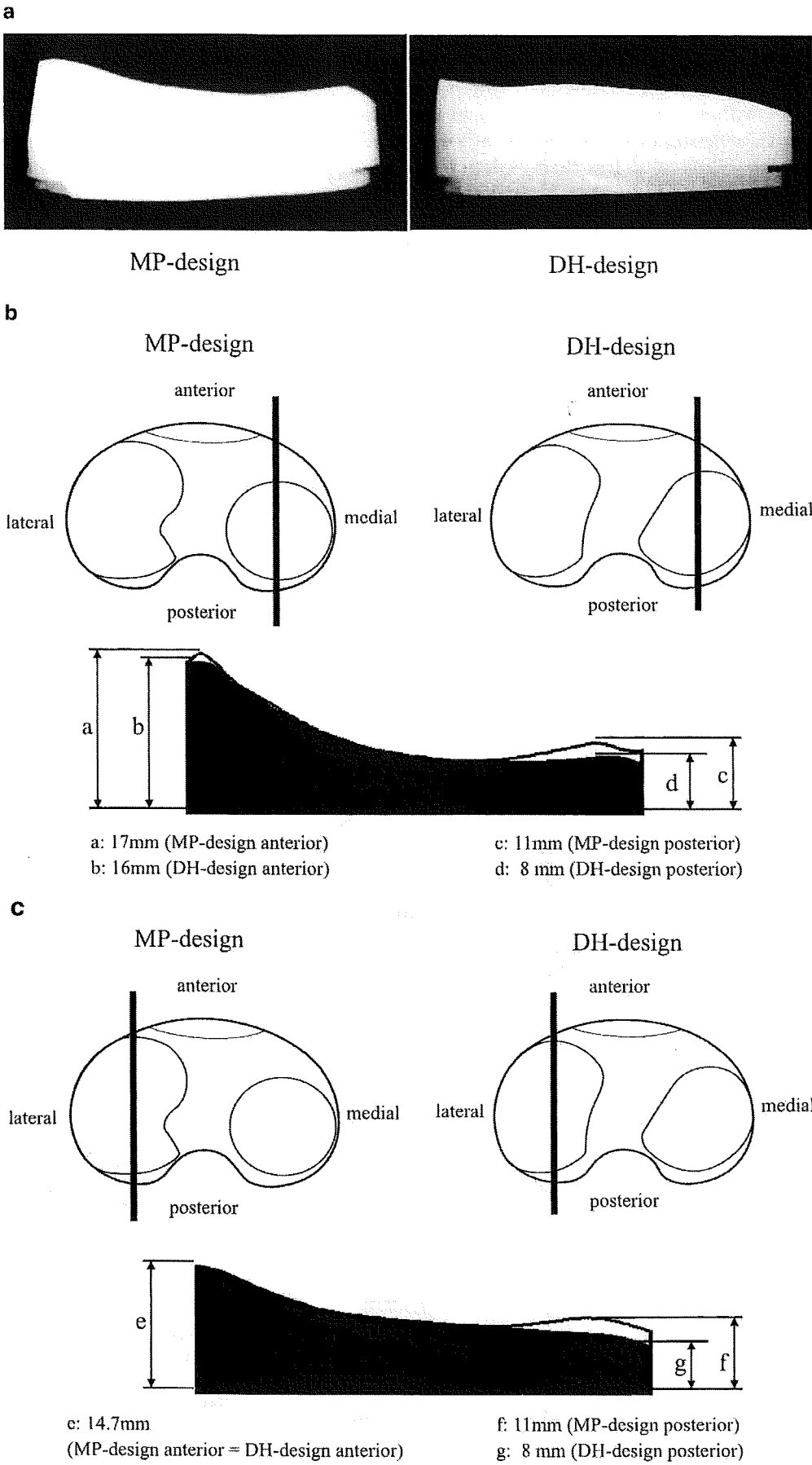


Fig. 1. Geometric characteristics of medial pivot design (DH-design) and double high design (DH-design). **a** Lateral view. **b** Cross-sectional geometry of the medial compartment. **c** Cross-sectional geometry of the lateral compartment

In this study, the anteroposterior motion of the ECP in the medial and lateral condyles was analyzed. Two-way analysis of variance (ANOVA) with within factors was used to analyze the effect of tibial insert geometry on the contact kinematics. The within factors were the aforementioned four different configurations. The significance level was set at a probability value less than 0.05.

Results

The MP-design showed bicondylar posterior translation under the PCL-retaining condition and medial pivot motion under the PCL-sacrificing condition. When the PCL was retained, the ECP of the medial compartment shifted posteriorly mainly more than 60° of knee flexion, and the ECP of the lateral compartment showed continuous posterior translation along knee flexion. The ECP of the medial compartment was located on the posterior lip of the ball-in-socket structure while demonstrating greater than 120° of knee flexion (Fig. 2a). The posterior translation of the ECP was 15.1 ± 3.1 mm (mean \pm SD) in the lateral compartment and $11.6 \pm$

2.9 mm in the medial, and no statistical difference was seen between either compartment (Fig. 3). After the PCL was sacrificed, the MP-design showed a typical medial pivot motion. The ECP of the medial compartment was located at almost the same point from 0° to 90° of knee flexion followed by a slight posterior translation of greater than 100° of flexion. On the other hand, the ECP of the lateral compartment showed continuous posterior translation along knee flexion (Fig. 2a). The posterior translation of the ECP was significantly greater in the lateral compartment (11.1 ± 3.8 mm) than that in the medial compartment (3.3 ± 2.5 mm) ($P = 0.022$) (Fig. 3).

The DH-design had basically the similar tracking pattern of the ECP as the MP-design under PCL-retaining conditions, which included a posterior shift of the medial ECP of greater than 60° of knee flexion and a continuous posterior translation of the lateral ECP. Both medial and lateral ECP shifted posteriorly on the posterior slope of the flexion path more than 120° of knee flexion (Fig. 2b). The posterior translation of the ECP was 14.5 ± 4.2 mm in the lateral compartment and 10.7 ± 3.8 mm in the medial compartment, and no statistical difference was found according to these results

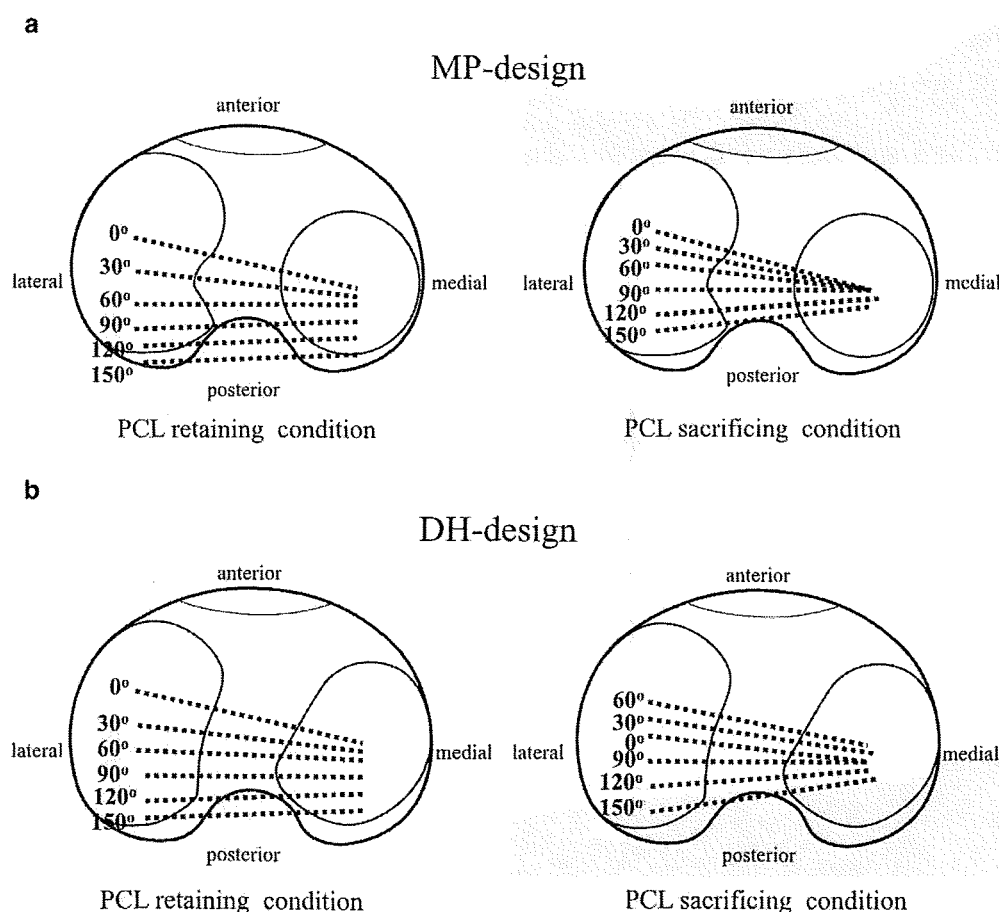


Fig. 2. Position movement of the estimated contact point (ECP). **a** MP-design. ECP of the medial compartment located the posterior lip of the ball-in-socket structure greater than 120° of knee flexion under posterior cruciate ligament (PCL)-retaining condition. **b** DH-design. ECP of the lateral compartment showed paradoxical anterior translation from 0° to 60° of knee flexion

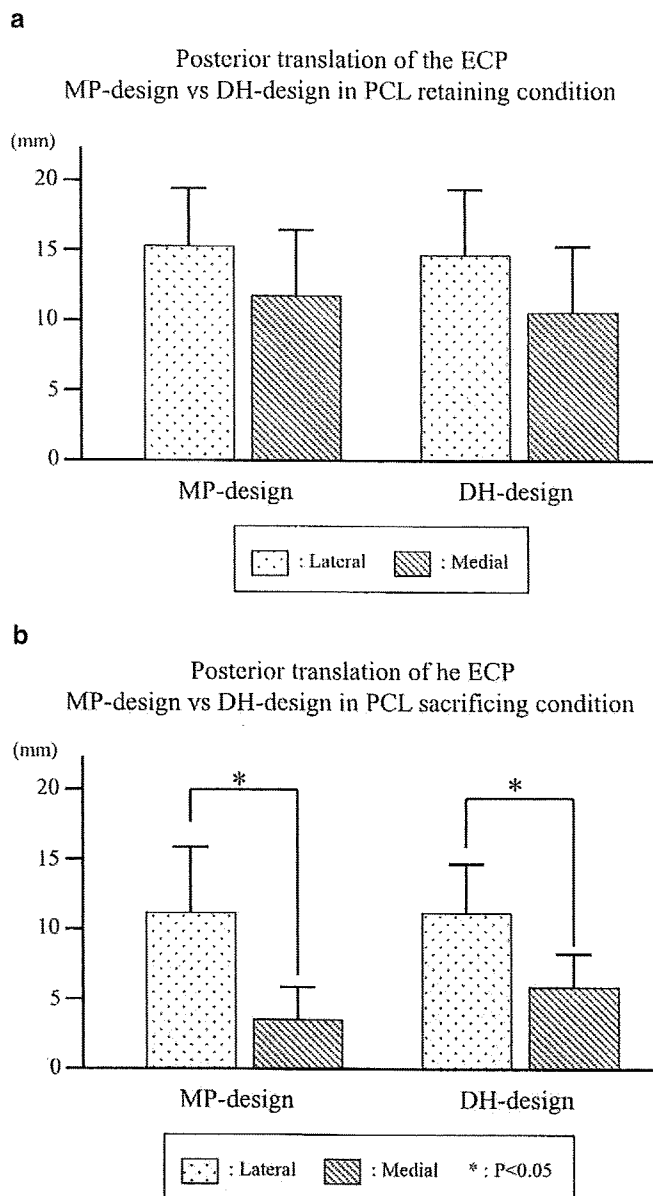


Fig. 3. Posterior translation of the ECP. **a** PCL-retaining condition. **b** PCL-sacrificing condition

(Fig. 3). The DH-design also showed a medial pivot motion after the PCL was sacrificed. The ECP of the medial compartment did not move from 0° to about 120° of knee flexion and then it slightly shifted to the posterior direction. In the lateral compartment, ECP showed paradoxical anterior translation from 0° to 60° of knee flexion followed by continuous posterior translation (Fig. 2b). The posterior translation of the ECP was 11.2 ± 3.6 mm in the lateral compartment and 5.5 ± 2.7 mm in the medial compartment, and then the posterior translation in the lateral ECP was significantly greater than that on the medial compartment ($P = 0.028$) (Fig. 3).

When comparing both designs, posterior translation of the ECP was not statistically different between the MP-design and DH-design under both PCL-retaining and PCL-sacrificing conditions.

Discussion

Currently, very few studies exist on the kinematic analysis of the medial pivot type TKA. Saari et al.¹⁸ evaluated the Samuelson total knee prosthesis and described that the medial spherical condyle stabilized anteroposterior motion. Schmidt et al.¹² studied the Advance Medial Pivot prosthesis using fluoroscopy and showed medial pivot motion during the stance phase of the gait cycle. Moonot et al.¹⁹ analyzed the Medial Rotation Knee with fluoroscopy and demonstrated medial pivot motion in a lunge motion.

In the present study, two different geometries of the polyethylene insert in the Advance Medial Pivot TKA were compared. The medial pivot geometry (MP-design) has a highly conformed "ball-in-socket" design to reproduce the medial pivot motion. On the other hand, the double high tibial insert (DH-design) is designed to achieve both medial pivot motion and posterior femoral rollback in deep knee flexion that will hopefully lead to more physiological kinematics and a better flexion angle. However, our data in the current study demonstrate that the contact kinematics by ECP did not substantially differ between the MP-design and the DH-design, especially in the deep flexion area greater than 120° of knee flexion. When the PCL was retained, both designs showed no medial pivot but did have bicondylar rollback, and, when the PCL was sacrificed, both designs showed no femoral rollback but typical medial pivot motion.

The first reason for this result is that medial ball-in-socket geometry is a highly conformed design and has an advantage in reproducing medial pivot motion, but it is insufficient for femoral rollback even if the posterior slope was made. The second reason is that femoral rollback is essentially controlled by the PCL, and this effect is stronger than that of the geometric conformity of the tibial insert as the MP-design and the DH-design under the PCL-retaining condition. Most et al.²⁰ analyzed femoral rollback after cruciate-retaining and stabilizing TKA and described that the cam-spine engagement structure played an important role in restoring posterior femoral rollback in the PCL-substituting TKA. However, the cam-post mechanism is not thought to reproduce medial pivot motion. Therefore, this study suggests that if we would reproduce both medial pivot motion and femoral rollback after TKA, a new concept and design of the tibial insert geometry will be needed.

In the MP-design, the ECP of the medial compartment located on the posterior edge of the ball-in-socket structure greater than 120° of flexion from bicondylar femoral rollback under the PCL-retained condition. Li et al.²¹ evaluated the in vivo tibiofemoral contact kinematics of a cruciate-retaining TKA and showed that the current component design did not allow the femoral condyle to roll off the polyethylene edge at high degrees of flexion because of the geometry at the posterior lip. Abnormal contact conditions between the polyethylene insert and metal tray in the MP-design may present some risk of polyethylene wear or limitations of knee flexion. On the other hand, the lateral ECP of the DH-design showed paradoxical anterior translation from 0° to 60° knee flexion under the PCL-sacrificing condition, possibly because of the lesser conformity of the medial ball-in-socket structure by decreasing the height of the anterior and posterior lip. Recently, short- to mid-term clinical results of the Advance Medial Pivot prosthesis were reported. However, none of the authors clearly described the treatment for the PCL.^{11,12,22} From the results of the present biomechanical study, it is recommended that the PCL should be sacrificed when the MP-design is used and retained when the DH-design is used.

There are several limitations because this is an in vitro cadaveric study. The first limitation is the number of specimens. Only seven cadaveric knees were evaluated in this study because it was difficult to obtain enough cadavers. Moreover, we selected knee joints of the same size for sequential evaluations, eliminating interspecimen variations. The second limitation is the loading condition. The load ratio of quadriceps and hamstring was close to physiological conditions; however, the actual amount of load was smaller than that of physiological condition as a result of the strength of the motion frame and load cell. In the near future, an in vivo kinematic study comparing the MP-design and the DH-design is needed.

The results of this study indicate that the ball-in-socket geometry in the MP-design has an advantage in reproducing medial pivot motion in the PCL-sacrificing condition and that the flexion path structure in the DH-design is effective for femoral rollback in the PCL-retaining condition. However, neither design is sufficient to reproduce medial pivot motion and posterior femoral rollback. Thus, a different design of tibial insert with a new concept is needed for more physiological kinematics after TKA.

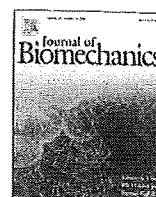
Acknowledgments. The authors thank Wright Medical Technology, Inc. for providing the TKA components.

The authors did not receive and will not receive any benefits or funding from any commercial party related directly or indirectly to the subject of this article.

References

1. Walker PS, Hake J. The load-bearing area in the knee joint. *J Biomech* 1972;5:581-9.
2. Iwaki H, Pinskerova V, Freeman MAR. Tibiofemoral movement 1: the shapes and relative movements of the femur and tibia in the unloaded cadaver knee. *J Bone Joint Surg* 2000;82B:1189-95.
3. Komistek RD, Dennis DA, Mahfouz M. In vivo fluoroscopic analysis of the normal human knee. *Clin Orthop Relat Res* 2003;410:69-81.
4. Nakagawa S, Kadota Y, Todo S, Kobayashi A, Sakamoto H, Freeman MAR, Yamano Y. Tibiofemoral movement 3: full flexion in the living knee studied by MRI. *J Bone Joint Surg* 2000;82B:1199-200.
5. Andriacchi TP, Galante JO, Fermier RW. The influence of total knee replacement design on walking and stair climbing. *J Bone Joint Surg* 1982;64A:1328-35.
6. Laskin RS. Joint line position restoration during revision total knee replacement. *Clin Orthop Relat Res* 2002;404:169-71.
7. Banks SA, Markovich GD, Hodge WA. In vivo kinematics of cruciate-retaining and -substituting knee arthroplasties. *J Arthroplasty* 1997;12:297-303.
8. Uvehammer J, Karrholm J, Brandsson S, Herberts P, Carlsson L, Regner L. In vivo kinematics of total knee arthroplasty: flat compared with concave tibial joint surface. *J Orthop Res* 2000;18:856-64.
9. Stiehl JB, Komistek RD, Dennis DA, Paxson RD, Horff WA. Fluoroscopic analysis of kinematics after posterior-cruciate-retaining knee arthroplasty. *J Bone Joint Surg* 1995;77B:884-9.
10. Dennis DA, Komistek RD, Colwell CE, Ranawat CS, Scott RD, Thornhill TS, Lapp MA. In vivo anteroposterior femoro-tibial translation of the total knee arthroplasty: a multicenter analysis. *Clin Orthop Relat Res* 1998;356:47-57.
11. Blaha JD. A medial pivot geometry. *Orthopedics* 2002;25:963-4.
12. Schmidt R, Komistek RD, Blaha JD, Penenberg BL, Maloney WJ. Fluoroscopic analysis of cruciate-retaining and medial pivot knee implants. *Clin Orthop Relat Res* 2003;410:139-47.
13. Li G, DeFrate LE, Zayontz S, Park SE, Gill TJ. The effect of tibiofemoral joint kinematics on patellofemoral contact pressures under simulated muscle loads. *J Orthop Res* 2004;22:801-6.
14. Gill TJ, DeFrate LE, Wang C, Carey CT, Zayontz S, Zarins B, Li G. The effect of posterior cruciate ligament reconstruction on patellofemoral contact pressures in the knee joint under simulated muscle loads. *Am J Sports Med* 2004;32:109-15.
15. Hayashi T, Kurokawa M, Miyasaka M, Aizawa A, Kanaki A, Saito A, Ishioka A. A high-resolution line sensor-based photostereometric system for measuring jaw movements in 6 d.o.f. *Front Med Biol Eng* 1994;6:171-86.
16. Nishino K, Hayashi T, Suzuki Y, Koga Y, Omori G. Accuracy verification of the photostereometric system KKN/1B developed for intraoperative measurement of knee movement immediately after total knee arthroplasty. *Front Med Biol Eng* 1999;9:261-73.
17. Omori G, Nishino K, Suzuki Y, Segawa H, Hayashi T, Koga Y. Intraoperative measurement of knee motion in total knee arthroplasty. *Knee* 2003;10:75-9.
18. Saari T, Uvehammer J, Carlsson LV, Herberts P, Regner L, Kärrholm J. Kinematics of three variations of the Freeman-Samuelson total knee prosthesis. *Clin Orthop Relat Res* 2003;410:235-47.
19. Moonot P, Mu S, Railton GT, Field RE, Banks SA. Tibiofemoral kinematic analysis of knee flexion for a medial pivot knee. *Knee Surg Sports Traumatol Arthrosc* 2009;17:927-34.
20. Most E, Zayontz S, Li G, Otterberg E, Sabbag K, Rubash HE. Femoral rollback after cruciate-retaining and stabilizing total knee arthroplasty. *Clin Orthop Relat Res* 2003;410:101-13.

21. Li G, Suggs J, Hanson G, Durbhakula S, Johnson T, Freiberg A. Three-dimensional tibiofemoral articular contact kinematics of a cruciate-retaining total knee arthroplasty. *J Bone Joint Surg* 2006;88A:395-402.
22. Shakespeare D, Ledger M, Kinzel V. Flexion after total knee replacement. A comparison between the Medial Pivot knee and a posterior stabilized implant. *Knee* 2006;13:371-3.



Short communication

Automated image registration for assessing three-dimensional alignment of entire lower extremity and implant position using bi-plane radiography

Koichi Kobayashi^{a,*}, Makoto Sakamoto^a, Yuji Tanabe^b, Akihiro Ariumi^c, Takashi Sato^c, Go Omori^d, Yoshio Koga^c^a Department of Health Sciences, Niigata University School of Medicine, 2-746 Asahimachi-dori, Chuo-ku, Niigata 951-8518, Japan^b Department of Mechanical Engineering, Niigata University, 2-8050 Ikarashi, Nishi-ku, Niigata 950-2181, Japan^c Department of Orthopaedic Surgery, Niigata Kobari Hospital, 3-27-11 Kobari, Nishi-ku, Niigata 950-2022, Japan^d Center for Transdisciplinary Research, Niigata University, 2-8050 Ikarashi, Nishi-ku, Niigata 950-2181, Japan

ARTICLE INFO

Article history:

Accepted 11 August 2009

Keywords:

Joint

3D position measurement

Accuracy

Lower leg Alignment

Biplanar radiography

ABSTRACT

An automated image-matching technique is presented to assess alignment of the entire lower extremity for normal and implanted knees and the positioning of implants with respect to bone. Sawbone femur and tibia and femoral and tibial components of a total knee arthroplasty system were used. Three spherical markers were attached to each sawbone and each component to define the local coordinate system. Outlines of the three-dimensional (3D) bone models and component computer-aided design (CAD) models were projected onto extracted contours of the femur, tibia, and implants in frontal and oblique X-ray images. Three-dimensional position of each model was recovered by minimizing the difference between the projected outline and the contour. Median values of the absolute error in estimating relative positions were within 0.5 mm and 0.6° for the femur with respect to the tibia, 0.5 mm and 0.5° for the femoral component with respect to the tibial component, 0.6 mm and 0.6° for the femoral component with respect to the femur, and 0.5 mm and 0.4° for the tibial component with respect to the tibia, indicating significant improvements when compared to manually obtained results.

© 2009 Elsevier Ltd. All rights reserved.

1. Introduction

Progression of osteoarthritis of the knee is related to alignment of the lower extremity. Postoperative lower extremity alignment is commonly considered an important factor in determining favorable kinematics to achieve success in total knee arthroplasty (TKA) (Singer et al., 1995). In addition, implant position with reference to bone is a critical factor affecting the long-term survival of TKA (Ritter et al., 1994).

Lower extremity alignment is currently assessed on a two-dimensional (2D) anteroposterior radiograph (Saleh et al., 1991; Sabharwal and Zhao, 2008) and may be influenced by position of the radiation source and orientation of the pelvis and lower extremity of the subject. Few studies have described the three-dimensional (3D) characteristics of lower extremity alignment during weight bearing (standing) (Cooke et al., 1994).

We have already developed a 3D lower extremity alignment assessment system with the subject in the standing position for pre-operative planning and postoperative alignment assessment for TKA (Sato et al., 2004, 2007). This system evaluates 3D

alignment by manually matching projections of 3D bone and component models with images of the entire lower extremity on frontal and oblique X-ray images, but is time-consuming and lowers the accuracy of position estimation. Automation of the image-matching process is thus desirable to reduce the burden of this laborious task and improve the accuracy of position estimation.

The purpose of the present study was to present an automated image-matching technique for assessing alignment of the entire lower extremity for normal and implanted knees and for assessing implant positioning with respect to bone. Examination of the accuracy of position estimation is also presented.

2. Materials and methods

Sawbone femur and tibia and femoral and tibial components of the Advance total knee system (Wright Medical Technology, Arlington, TN, USA) were used. Three spherical acrylic markers (diameter, 25 mm) were attached to the femur and tibia and three spherical stainless markers (diameter, 5 mm) were attached to femoral and tibial components. Computed tomography (CT) was performed for the femur and tibia with these markers to reconstruct 3D surface models. Local coordinate systems of femoral and tibial surface models were defined based on central coordinates of markers attached to the surface models using a coordinate system creator (ModelViewer, LEXI, Tokyo, Japan). For components, computer-aided design (CAD) models were provided by the manufacturer. Using a 3D model editor (Magics 11, Materialise, Leuven, Belgium), 5 mm diameter spheres were placed at the actual positions of the markers measured by a 3D coordinate

* Corresponding author. Tel./fax: +81 25 227 0935.

E-mail address: kobayasi@clg.niigata-u.ac.jp (K. Kobayashi).

measuring machine (BH504, Mitutoyo, Kawasaki, Japan) with an accuracy of 1.0 μm . This machine measures 3D coordinates of the subject using a probe. A local coordinate system for each CAD model was then defined based on the central coordinates of the sphere models.

Four relative positions were obtained between femur and tibia, femoral component and tibial component, femoral component and femur, and tibial component and tibia. The femur and tibia were securely fixed at full extension using an external fixation device (Fig. 1A). The 3D position for each sawbone was determined based on central coordinates of the markers measured using the 3D coordinate measuring machine. Both femur and tibia were removed from the fixation device after biplanar X-ray exposure, which is described later, and femoral and tibial components were installed (Fig. 1B and C). The 3D position of each pair of bone and component was measured using the 3D coordinate measuring machine and biplanar X-ray images were taken. Each component was then removed and placed in a different position than before, and biplanar X-ray images were again taken. This process was performed a total of 4 times. The implanted femur and tibia were fixed again using the external fixation device (Fig. 1D). The 3D position measurement of each bone and biplanar X-ray exposure were performed on three different relative positions between the femur and tibia. Both components were then removed from both bones and fixed using a custom device (Fig. 1E). The 3D position measurement and biplanar X-ray exposure were performed on four relative positions between the two components. This separate measurement was performed due to the difficulty in touching the markers attached

to the components with the probe when the implanted femur and tibia were fixed as shown in Fig. 1D. Note that one of the four relative positions between the femur and tibia was obtained before femoral and tibial components were installed.

A biplanar computed radiography system was used to capture frontal and oblique X-ray images. The rotation table was positioned at 0° and 60° relative to the optical axis of the X-ray source (Fig. 2). For each table position, X-ray tube calibration was performed beforehand to determine the projection matrix (Faugeras, 1993). The projection matrix provides 3D positioning of the focus of the X-ray source, and the image plane with respect to the calibration frame, enabling projections of 3D objects to be replicated on the image plane following X-ray exposure (Fig. 3). Contours of the femur, tibia and implants in biplanar radiographs were detected using the method described by Canny (1986). Projected outline points of each 3D model were the finite edge points of the 2D shadow created from the projections of all visible triangular surfaces of the 3D model.

For the i th point of the object contour, \mathbf{p}_i , the closest point of the projected outline of the corresponding model, \mathbf{q}_i , was examined. Distance between the two points was summed over all object contour points and subsequently normalized by the total number of points, N . Object function F represents the sum of normalized distances determined from frontal and oblique images:

$$F = \sum_{i=1}^{N^{FR}} |\mathbf{p}_i^{FR} - \mathbf{q}_i^{FR}| / N^{FR} + \sum_{i=1}^{N^{OB}} |\mathbf{p}_i^{OB} - \mathbf{q}_i^{OB}| / N^{OB}, \quad (1)$$

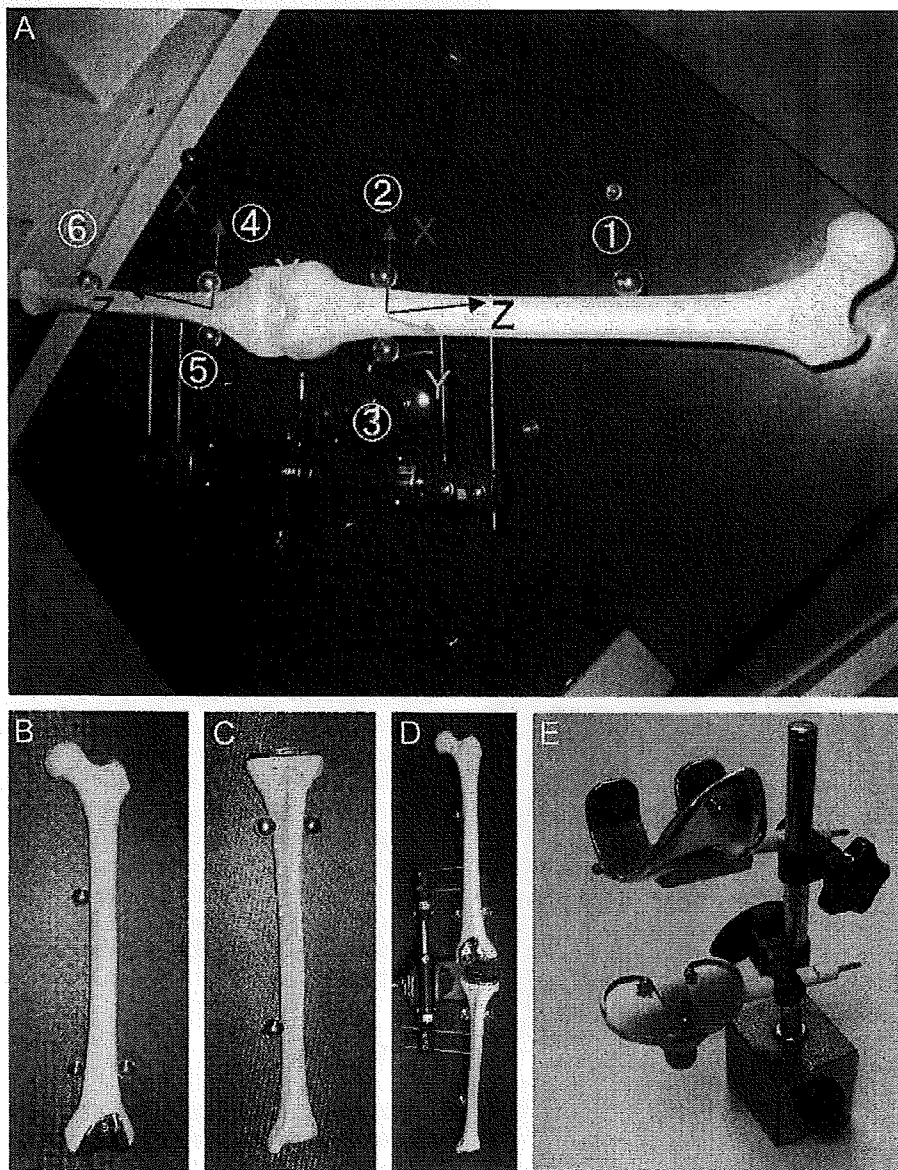


Fig. 1. Set-up for measurement of relative position. (A) The sawbone femur and tibia were immobilized using an external fixation device. (B) Femur with the femoral component attached. (C) Tibia with tibial component attached. (D) The implanted femur and tibia were immobilized using an external fixation device. (E) Femoral and tibial components were immobilized using a custom fixation device.

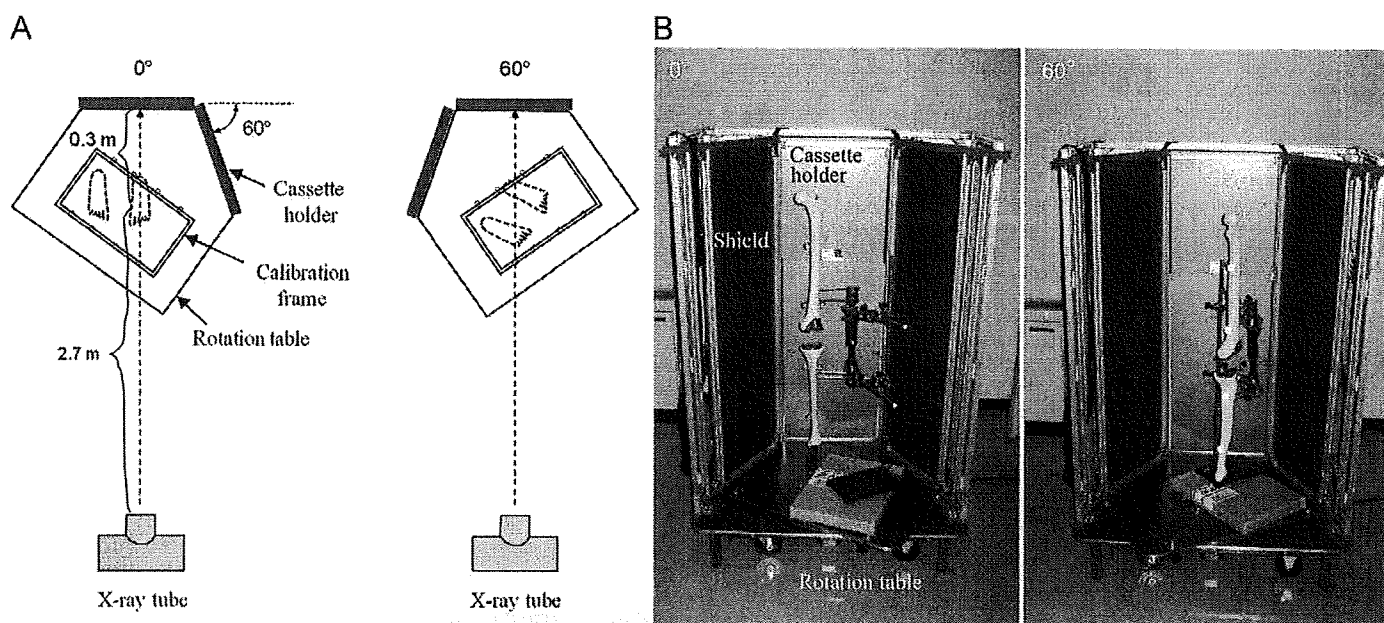


Fig. 2. Calibration set-up for the rotation table for bi-plane radiography (A). An acrylic frame with 72 spherical stainless markers attached was used for calibration. Half of the 72 markers were attached to the frontal surface, and the other half attached to the back surface to cover the volume of the lower extremity ($270 \times 180 \times 800 \text{ mm}^3$). The 3D positions of these markers were measured using the 3D coordinate measuring machine. The two cassettes rotated with the table, while normal directions were set to align with the optical axis. Each cassettes contained three $14 \times 14 \text{ in}^2$ imaging plates that were to be digitized in 8-bit gray intensity with 0.2 mm resolution (FCR; Fuji, Tokyo, Japan). Diameters of markers were 4 mm for frontal surface markers and 3 mm for back surface markers. This discrepancy was used to emphasize differences in projected size of the marker in radiographs, to facilitate identification of markers. Footprints indicate the standing position of the subject, where the left leg is being imaged. The repeatability (standard deviation) of table positioning between the table positioned at 0° and 60° was $\pm 0.3^\circ$ ($n=5$). Fixed femur and tibia were X-rayed at 0° and 60° (B).

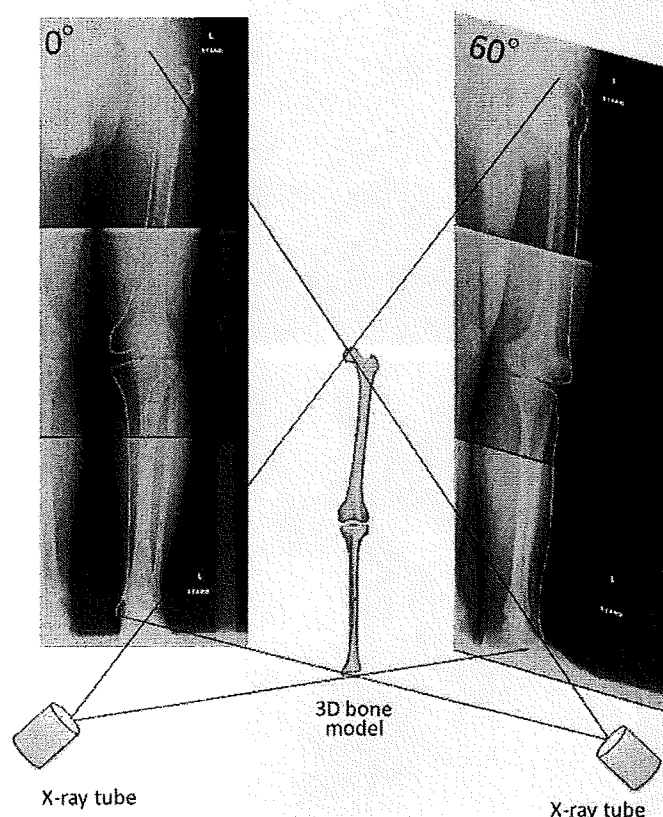


Fig. 3. Synthetic biplanar X-ray system. Projected outline points of each 3D model were the finite edge points of the 2D shadow created from the projections of all visible triangular surfaces of the 3D model.

where superscripts *FR* and *OB* denote the values standing for frontal and oblique images. The 3D position of each model (full 6-degrees of freedom (DOF) parameters) was recovered by minimizing F using the downhill simplex algorithm (Nelder and Mead, 1965). Ten sets of initial 6-DOF parameters for minimization were arbitrarily chosen from $\pm 5.0^\circ$ and $\pm 5.0 \text{ mm}$ of true values of each relative position. The minimization procedure terminates if either the number of iterations exceeds 500 or the relative change in F is below 0.00005. Manual image matching was also performed from 10 sets of initial 6-DOF parameters arbitrarily ranging within $\pm 5.0^\circ$ and $\pm 5.0 \text{ mm}$ of true values.

3. Results

Mean values, standard deviations, and median values of absolute errors in relative position parameters determined by manual and automated methods are listed in Table 1. The automated method produced significantly better results for all position parameters, except for rotation about the x -axis and translation along the x -axis at the relative position of the femoral component with respect to the femur (The Wilcoxon signed-rank test). The running times for automated minimization on a Windows XP PC (XEON processor, 3 GHz, 2 GB RAM) of about 270 s for bone and 30 s for components were reduced from those for the manual method (about 600 s for bone and 300 s for components).

4. Discussion

Image-based techniques for direct 3D measurements of bone and implant positions are a practical approach, since the insertion of markers into bone is not required. Our automated method offered better accuracy and time efficiency than the manual method. However, the present results were less accurate than those obtained by de Bruin et al. (2008) and Li et al. (2004),

Table 1Mean, SD, and median value of absolute error for estimating 6-DOF parameters of relative positions ($n=40$).

Relative position			Rotation			Translation		
			x (°)	y (°)	z (°)	x (mm)	y (mm)	z (mm)
Femur/tibia	Manual	Mean	0.6	0.5	1.5	1.0	1.6	1.1
		SD	0.4	0.4	1.0	0.8	1.4	0.9
		Median	0.4	0.4	1.3	0.8	1.4	0.9
	Automated	Mean	0.2	0.3	0.7	0.3	0.5	0.5
		SD	0.2	0.2	0.4	0.3	0.3	0.2
		Median	0.1	0.3	0.6	0.1	0.5	0.5
		p	< 0.001	0.005	0.001	< 0.001	< 0.001	< 0.001
Femoral component/tibial component	Manual	Mean	0.8	0.9	1.0	1.1	0.6	1.1
		SD	0.7	0.5	0.7	0.7	0.4	0.7
		Median	0.6	1.0	0.9	1.1	0.6	1.0
	Automated	Mean	0.3	0.4	0.4	0.5	0.3	0.5
		SD	0.2	0.3	0.3	0.4	0.2	0.3
		Median	0.3	0.3	0.5	0.4	0.4	0.5
		p	< 0.001	< 0.001	< 0.001	< 0.001	< 0.001	< 0.001
Femoral component/femur	Manual	Mean	0.7	1.2	1.0	0.9	1.7	1.2
		SD	0.4	0.7	0.8	0.8	0.9	1.0
		Median	0.6	0.4	0.5	0.6	0.5	0.3
	Automated	Mean	0.6	0.5	0.5	0.7	0.6	0.5
		SD	0.3	0.3	0.3	0.4	0.5	0.4
		Median	0.6	0.4	0.5	0.6	0.5	0.3
		p	0.170	< 0.001	0.011	0.687	< 0.001	0.001
Tibial component/tibia	Manual	Mean	0.5	1.8	0.6	0.9	1.3	1.0
		SD	0.3	1.0	0.4	0.6	1.1	0.8
		Median	0.5	1.9	0.5	0.7	1.1	0.8
	Automated	Mean	0.2	0.6	0.4	0.3	0.4	0.5
		SD	0.2	0.5	0.2	0.2	0.3	0.3
		Median	0.1	0.4	0.4	0.3	0.4	0.5
		p	< 0.001	< 0.001	0.042	< 0.001	< 0.001	0.001

 p -Values indicate significance of the difference between automatically obtained results and manually obtained results.

probably due to small differences in positions of the rotation table and cassette holder from those set during camera calibration. Conversely, our results for the standard deviation of estimating implant position in reference to bone were equivalent to that determined using postoperative CT (Jazrawi et al., 2000).

Cooke et al. (1994) provided quantitative lower limb alignment parameters in the coronal and sagittal planes using anteroposterior and lateral radiographs taken using a turntable, but did not quantify the axial parameters because the axial geometry of the lower extremity was not reconstructed in three dimensions. The present method would therefore enable more reliable analysis of load-bearing characteristics across the knee joint.

The use of CT may lower the applicability of our method, due to concerns about exposure to radiation. However, although the effective radiation dose of 6 mSv from CT is about 10 times larger than that required for radiography, this dose is comparable to the annual effective dose from natural background radiation of about 3 mSv (Mettler et al., 2008). Although magnetic resonance imaging can be regarded as an alternative method, imaging the entire length of the femur or tibia is currently difficult. The choice of CT is thus relevant for the purposes of this method.

When applying this method to patients, care must be taken to prevent body motion during X-ray exposure. In addition, since the soft tissues surrounding bone may reduce the reliability of contour extraction from bone, studies examining actual patients are needed to clarify the clinical applicability of this procedure.

In conclusion, the present study demonstrates the accuracy of relative 3D position estimation using an automated image-matching technique in experiments with bi-plane radiographs of sawbones and TKA components.

Conflict of interest statement

None.

Acknowledgements

Funding from the Japan Society for the Promotion of Science (Grant-in-Aid for Scientific Research B19360046) is acknowledged.

References

- Canny, A., 1986. A computational approach to edge detection. *IEEE Transactions on Pattern Analysis and Machine Intelligence* PAMI 8 (6), 679–698.
- Cooke, T.D.V., Li, J., Scudamore, R.A., 1994. Radiographic assessment of bony contributions to knee deformity. *Orthopedic Clinics of North America* 25 (3), 387–393.
- de Bruin, P.W., Kaptein, B.L., Stoel, B.C., Reiber, J.H.C., Rozing, P.M., Valstar, E.R., 2008. Image-based RSA: Roentgen stereophotogrammetric analysis based on 2D–3D image registration. *Journal of Biomechanics* 41, 155–164.
- Faugeras, O., 1993. *Three-Dimensional Computer Vision: A Geometric Viewpoint*. MIT Press, Cambridge.
- Jazrawi, L.M., Birdzell, L., Kummer, F.J., Di Cesare, P.E., 2000. The accuracy of computed tomography for determining femoral and tibial total knee arthroplasty component rotation. *Journal of Arthroplasty* 15 (6), 761–766.
- Li, G., Wuerz, T.H., DeFrate, L.E., 2004. Feasibility of using orthogonal fluoroscopic images to measure in vivo joint kinematics. *Journal of Biomechanical Engineering* 126, 314–318.
- Mettler, F.A., Huda, W., Yoshizumi, T.T., Mahesh, M., 2008. Effective doses in radiology and diagnostic nuclear medicine: a catalog. *Radiology* 248 (1), 254–263.
- Nelder, J.A., Mead, R., 1965. A simplex method for function minimization. *Computer Journal* 7, 308–313.
- Ritter, M.A., Faris, P.M., Keating, E.M., Meding, J.B., 1994. Postoperative alignment of total knee replacement. Its effect on survival. *Clinical Orthopaedics and Related Research* 299, 153–156.

- Sabharwal, S., Zhao, C., 2008. Assessment of lower limb alignment: supine fluoroscopy compared with a standing full-length radiograph. *Journal of Bone and Joint Surgery (American)* 90, 43–51.
- Saleh, M., Harriman, P., Edwards, D.J., 1991. A radiological method for producing precise limb alignment. *Journal of Bone and Joint Surgery (British)* 73, 515–516.
- Sato, T., Koga, Y., Omori, G., 2004. Three-dimensional lower extremity alignment assessment system. Application to evaluation of component position after total knee arthroplasty. *Journal of Arthroplasty* 19 (5), 620–628.
- Sato, T., Koga, Y., Sobue, T., Omori, G., Tanabe, Y., Sakamoto, M., 2007. Quantitative 3-dimensional analysis of preoperative and postoperative joint lines in total knee arthroplasty. *Journal of Arthroplasty* 22 (4), 560–568.
- Singerman, R., Heiple, K.G., Davy, D.T., Goldberg, V.M., 1995. Effect of tibial component position on patella strain following total knee arthroplasty. *Journal of Arthroplasty* 10 (5), 651–656.

Pulmonary Function Analysis of Japanese Athletes: Possibly Even More Asthmatics in the Field

Junta Tanaka^{1,2}, Takashi Hasegawa⁴, Toshiyuki Koya³, Masao Hashiba¹, Go Omori⁵,
Fumitake Gejyo³, Eiichi Suzuki⁴ and Masaaki Arakawa¹

ABSTRACT

Background: The prevalence of bronchial asthma (BA) in youth is increasing in Japan, but very few athletes are reported to be affected with BA. The aim of this study is to analyze pulmonary function test (PFT) in athletes from the aspect of BA retrospectively.

Methods: Medical history questionnaires of 2111 athletes (male: 1549, female: 562) were reviewed. All athletes participated in the institute's athletic test for the first time, from April 2003 through March 2006. Athletes were categorized into three groups; current-BA confirmed and treated by the physician, possible-BA according to the allergic history and/or BA symptoms, and non-BA that is neither of the above two groups. The PFT data were then analyzed.

Results: There were 24 current-BA (1.1%), 137 possible-BA (6.5%), and 183 cases with a past history of BA (PH; 8.7%). Percent of predicted forced expiratory volume in 1 second (%FEV₁) and of predicted peak expiratory flow rate (%PEF) in current-BA ($86.2 \pm 17.7\%$ and $81.6 \pm 19.1\%$, respectively) and possible-BA ($84.7 \pm 14.6\%$ and $81.2 \pm 17.3\%$, respectively) were significantly lower than those in non-BA ($93.9 \pm 13.7\%$ and $93.8 \pm 19.8\%$, respectively), without any significant difference between current-BA and possible-BA. Athletes with PH show impaired obstructive indices; even in non-BA with PH showed lower %FEV₁ ($91.3 \pm 13.9\%$, $p < 0.05$) and %PEF ($86.8 \pm 17.8\%$, $p < 0.001$) than non-BA without PH ($94.0 \pm 13.7\%$ and $94.2 \pm 19.9\%$, respectively).

Conclusions: The incidence of BA in Japanese athletes may be higher than currently recognized. More intervention is encouraged for the diagnosis of BA, to avoid any fatal asthma during sports by initiating preventive therapy.

KEY WORDS

asthma, athletic injuries, exercise-induced asthma, exercise-induced bronchospasm, pulmonary function test

INTRODUCTION

A negligible number of Japanese athletes requested the use of an inhaled beta agonist (IBA) at recent Olympic Games¹; only one out of 268 athletes from Japan applied for permission at the Sydney Games, where 112 out of 594 athletes from the United States of America notified the use. This low prevalence of notification by Japanese athletes may be partly due to

the relatively low prevalence of bronchial asthma (BA) patients in Japan.

The prevalence of BA among Japanese children has increased by 3% in the last 20 years, and two recently conducted government surveillances have revealed the rate in school-age children to be 5.7 and 7.6%. In 2003, the Global Initiative for Asthma (GINA) also reported a similar rate of 6.7% as the prevalence of BA symptoms in Japanese school-age children,

¹Niigata Institute for Health and Sports Medicine, ²Bioscience Medical Research Center, ³Department of Medicine (II), ⁴Department of General Medicine, Niigata University Medical and Dental Hospital and ⁵Center of Transdisciplinary Research, Niigata University, Niigata, Japan.

Authors' contributions: TH, ES and MA made conception and design of this paper. MH, GO, and FG performed the administrative support. MH and MA provided the study materials or patients. JT, TH and MH contributed to collection and assembly of data. JT, TH and TK performed the data analysis and interpretation. JT and TH

wrote the manuscript. All the authors have read and approved the final manuscript.

Correspondence: Junta Tanaka, MD, Bioscience Medical Research Center, Niigata University Medical and Dental Hospital, 1-754 Asahimachi-dori, Chuo-ku, Niigata-city, Niigata 951-8520, Japan.

Email: juntatnk@med.niigata-u.ac.jp

Received 2 March 2009. Accepted for publication 3 July 2009.

©2010 Japanese Society of Allergology

Table 1 Medical questionnaire regarding history and symptoms of bronchial asthma and allergy

BA † history:

1. Is the athlete on the follow-up of BA at the clinic? (current-BA)
2. Has the athlete been diagnosed as BA during the childhood? (PH ‡)

BA symptoms:

3. Has the athlete ever been diagnosed as allergic disease other than BA?
4. Has any of the family (siblings or parents) been diagnosed as BA?
5. Does the athlete experience wheezing, chest tightness, breathlessness, cough, or excess of sputum at night or early in the morning?
6. Does the athlete experience wheezing, chest tightness, breathlessness, cough, or excess of sputum after exposure to the certain airborne substances (allergens or pollutants)?
7. Does the athlete experience wheezing, chest tightness, breathlessness, cough, or excess of sputum during and after the exercise?
8. Does the athlete experience wheezing, chest tightness, breathlessness, cough, or excess of sputum as the seasonal exacerbation?
9. Do the athlete's colds take more than 14 days to clear up?
(One point for each "yes" answer to question 3 through 9, and the athlete is considered possible-BA if the score is three or greater.)

† BA, bronchial asthma.

‡ PH, past history of asthma.

which is below the rate for the United States of America, 10.9%.²

The prevalence of BA in athletes is higher than in the general population,³⁻⁷ and considering the difference in prevalence between Japan and the United States of America shown above, many Japanese athletes possibly have undiagnosed BA; the percentage of Japanese athletes who applied for the use of IBA is too low referring to the prevalence of BA among Japanese children. Moreover, there is no published report so far, regarding the prevalence of asthma-related disorders among Japanese athletes.

Thus, we have decided to analyze the baseline pulmonary function test (PFT) data regarding the BA background of athletes, since our medical questionnaire for the health check-ups included the BA-related history and symptoms. Recent studies show that the medical questionnaires or interviews are not reliable in identifying the exercise-induced bronchospasm (EIB).⁸ EIB should be documented by evaluating the PFT in response to appropriate exercise or provocation tests. However, medical history is still a helpful guide in the clinical diagnosis of BA, and can be used in screening of BA regardless of EIB.

The primary aim of this study was to analyze screening PFT of Japanese athletes from the aspect of BA, by the groups categorized through the scoring of a medical questionnaire regarding asthma symptoms and allergic history.

METHODS

STUDY DESIGN

We conducted a cross-sectional retrospective study of regional elite athletes who participated in their first athletic test performed at the Niigata Institute for Health and Sports Medicine, from April 2003 through

March 2006. A total of 2111 athletes (1549 males, 562 females, age 18.0 ± 4.1 years) were included in this study. The data from screening tests were collected during the preparticipation health check-ups, including a medical questionnaire focused on history and symptoms of BA and allergy (Table 1), and baseline PFT. The study procedures including participant's anonymity preservation were approved by the Ethical Committee of the Niigata Institute for Health and Sports Medicine in accordance with the principles embodied in the Declaration of Helsinki, and each subject, parents, or legal guardian provided written informed consent.

ASTHMA AND ALLERGY QUESTIONNAIRE

A detailed BA and allergy history and review of symptoms were obtained using a medical questionnaire as shown in Table 1. The questionnaire consisted of 9 items relevant to the diagnosis of BA, also referring to the medical history consideration shown by GINA,⁹ and an athlete was categorized as current-BA, possible-BA, or non-BA. The athlete was considered current-BA if BA was confirmed and treated by the physician, possible-BA if scoring 3 or more items for the allergic history and/or BA symptoms, and non-BA if the athlete was neither current-BA nor possible-BA. Possible-BA, however, was defined as above in this study to categorize athletes into groups, simply for the sake of convenience to analyze baseline PFT retrospectively.

PULMONARY FUNCTION TEST BY SPIROMETRY

A baseline PFT by spirometry was performed for all participants. The best value from three measurements of vital capacity (VC), forced vital capacity (FVC), forced expiratory volume in one second

Table 2 Categorical characteristics of the participants

	Number (%)	Male/Female
Total participants	2111 (100)	1549/562
Current-BA	24 (1.1)	17/7
(PH ⁺)	20	15/5
Possible-BA	137 (6.5)	97/40
(PH ⁺)	48	40/8
Non-BA	1950 (92.4)	1435/515
(PH ⁺)	115	80/35

(FEV₁), peak expiratory flow (PEF) were used and recorded by a spirometer, SpiroSift SP-470 (Fukuda Denshi, Tokyo, Japan.). Predicted values were calculated by the standard formulae originally programmed in the spirometer.

DATA ANALYSIS AND STATISTICS

Percent of predicted FEV₁ (%FEV₁), percent of predicted PEF (%PEF), and FEV₁/FVC (FEV₁%) were analyzed for each category of athletes, current-BA, possible-BA, and non-BA. The data were further analyzed according to the past history of asthma (PH) status. Values for all measurements are expressed as mean (%) ± SD.

Kruskal-Wallis test, and Mann-Whitney *U* tests were used to determine the levels of difference between all groups. Significance was assumed at *p*-values of <0.05.

RESULTS

There were 24 current-BA (1.1%), 137 possible-BA (6.5%), and 1950 non-BA (92.4%) cases. In 183 cases of PH (8.7%), there were 20 current-BA, 47 possible-BA, and 116 non-BA cases. Considering the rate of PH, cumulative morbidity of BA was estimated as 8.9%. The difference between male and female athletes was not discussed in this study, because 562 female athletes were analyzed, and there were only seven cases with current-BA and 40 cases with possible-BA, which resulted in numbers that were too few to see any significance (Table 2).

As shown in Figure 1, current-BA showed a significantly decreased %FEV₁ (current-BA vs. non-BA; $86.2 \pm 17.7\%$ vs. $93.9 \pm 13.7\%$), %PEF ($81.6 \pm 19.1\%$ vs. $94.3 \pm 26.2\%$) and FEV₁% ($84.6 \pm 8.3\%$ vs. $89.0 \pm 5.8\%$) compared to non-BA, even under the relevant treatment ($p < 0.001$). Interestingly, possible-BA is also significantly decreased in pulmonary function parameters compared to non-BA (possible-BA vs. non-BA; $84.7 \pm 14.6\%$ vs. $93.9 \pm 13.7\%$ in %FEV₁, $81.2 \pm 17.3\%$ vs. $94.3 \pm 26.2\%$ in %PEF, and $84.9 \pm 7.5\%$ vs. $89.0 \pm 5.8\%$ in FEV₁%, all with $p < 0.001$, respectively). However, there was no significant difference between current-BA and possible-BA (Fig. 1). %VC, which is one of restrictive indices in PFT, was of no difference among all groups (data not shown).

To determine the influence of PH on pulmonary function, comparison between groups either with or without PH was performed. Among all participants, the group with PH (PH⁺) showed decreased pulmonary function parameters compared to the group without PH (PH⁻) (PH⁺ vs. PH⁻; $89.9 \pm 14.3\%$ vs. $93.5 \pm 14.0\%$ in %FEV₁, $p < 0.001$, $87.2 \pm 17.8\%$ vs. $93.4 \pm 20.0\%$ in %PEF, $p < 0.005$, $86.8 \pm 6.6\%$ vs. $88.8 \pm 6.0\%$ in FEV₁%, $p < 0.001$). In regard to non-BA, PH⁺ also revealed decreased airway function compared to PH⁻ (PH⁺ vs. PH⁻; $91.3 \pm 13.9\%$ vs. $94.0 \pm 13.7\%$ in %FEV₁, $p < 0.05$, $86.8 \pm 17.8\%$ vs. $94.2 \pm 19.9\%$ in %PEF, $p < 0.001$, $87.3 \pm 6.0\%$ vs. $89.1 \pm 5.8\%$ in FEV₁%, $p < 0.005$). In contrast, when the samples are limited to possible-BA, the findings were vice versa; PH⁻ had decreased airway function in comparison with PH⁺ (PH⁺ vs. PH⁻; $87.6 \pm 13.1\%$ vs. $83.2 \pm 15.2\%$ in %FEV₁, $p = 0.104$, $89.0 \pm 17.6\%$ vs. $77.1 \pm 15.7\%$ in %PEF, $p < 0.005$, $86.8 \pm 6.8\%$ vs. $84.0 \pm 7.7\%$ in FEV₁%, $p < 0.05$). And even in 24 current-BA, though sample numbers were too small to make conclusions, PH⁻ in this category had a tendency for decreased airway function compared to PH⁺ except for FEV₁% (PH⁺ vs. PH⁻; $87.0 \pm 18.5\%$ vs. $81.6 \pm 14.4\%$ in %FEV₁, $84.2 \pm 19.5\%$ vs. $67.3 \pm 10.8\%$ in %PEF, $84.5 \pm 8.5\%$ vs. $85.1 \pm 7.8\%$ in FEV₁%) (Table 3).

DISCUSSION

The study by Hammerman, *et al.* showed that there were 5.7% BA or EIB among American high school athletes, and another 6.1% were identified as having undiagnosed BA.¹⁰ In the present study, although the athletes defined as possible-BA were not medically confirmed as BA at the time of visit, the obstructive indices of PFT showed similar results compared with current-BA. These data suggest that a considerable number of these athletes may also have undiagnosed BA.

A recent nation-wide survey on the health and welfare status by the Japanese government revealed that 71.3% of the all-age patients with BA symptoms were under antiasthmatic medication, but only 54.6% of such patients aged between 15 and 34 years were under relevant treatment.¹¹ Of 161 athletes with either current-BA or possible-PA in our study, less than 15% of them were current-BA who were on medication, thus indicating that the prevalence of untreated BA may also be higher among athletes. Importantly, a 7-year observation of BA deaths by Becker, *et al.* report that of 61 casualties during sport activities, 55 cases had mild intermittent or persistent BA before their fatal attack, and that only 3 of them used long-term controller medication.¹² Although most of the non-current-BA athletes tested in our study had little respiratory symptoms during and after the usual exercise, the undiagnosed BA should thoroughly be detected, in order to avoid any future BA deaths related to exercise and sport activities.

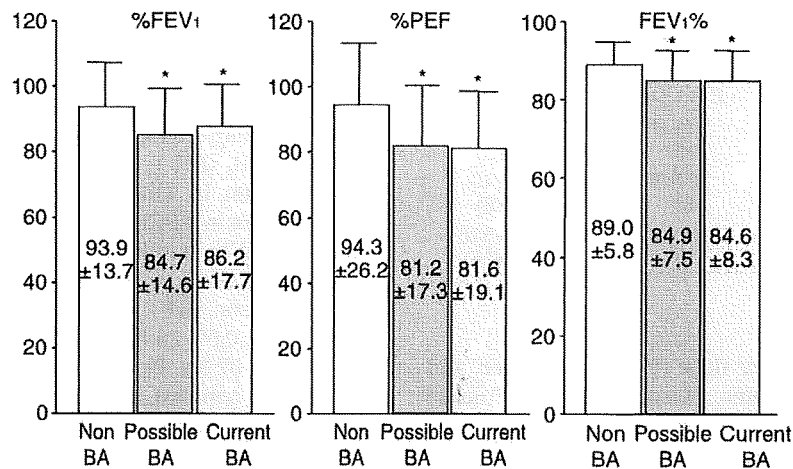


Fig. 1 Obstructive indices of pulmonary function tests (%FEV₁, %PEF, and FEV₁%) in athletes. Data express mean (%) ± SD. * $p < 0.001$ by the Kruskal-Wallis test.

Table 3 Obstructive indices of pulmonary function test in athletes with or without past history of asthma.

	%FEV ₁ (%)	%PEF (%)	FEV ₁ % (%)
All participants			
PH ⁺ (n = 183)	89.9 ± 14.3***	87.2 ± 17.8**	86.8 ± 6.6***
PH ⁻ (n = 1928)	93.5 ± 14.0	93.4 ± 20.0	88.8 ± 6.0
Current-BA			
PH ⁺ (n = 20)	87.0 ± 18.5†	84.2 ± 19.5†	84.5 ± 8.5†
PH ⁻ (n = 4)	81.6 ± 14.4	67.3 ± 10.8	85.1 ± 7.8
Possible-BA			
PH ⁺ (n = 48)	87.6 ± 13.1	89.0 ± 17.6**	86.8 ± 6.8*
PH ⁻ (n = 89)	83.2 ± 15.2	77.1 ± 15.7	84.0 ± 7.7
Non-BA			
PH ⁺ (n = 115)	91.3 ± 13.9*	86.8 ± 17.8***	87.3 ± 6.0**
PH ⁻ (n = 1835)	94.0 ± 13.7	94.2 ± 19.9	89.1 ± 5.8

Data express mean ± SD, * $p < 0.05$, ** $p < 0.005$, *** $p < 0.001$; compared with PH⁻.

† Insufficient sample numbers for statistical analysis.

Another important message is derived from the results concerning the influence of PH on pulmonary function. The present study has shown that athletes with PH, who were even considered as non-BA, had impaired pulmonary function indices, suggesting they may not have fully recovered from their childhood asthma. In general, it has been reported that up to 70% of BA patients in childhood lose their symptoms during puberty.^{13,14} Oswald, *et al.* conducted 28-year follow-up study for mild asthmatics in childhood, and suggested that airway obstruction or hyperresponsiveness of the patients would be restored normally even if they did not use inhaled corticosteroids.¹⁵ On the contrary, Agertoft, *et al.* showed that a delay in the introduction of inhaled corticosteroids resulted in incomplete recovery of pulmonary function.¹⁶ Moreover, Pederson, *et al.* reported that early

intervention with sufficient doses of inhaled corticosteroids could cure the disease with no recurrence.¹⁷ In this regard, our data may also indicate the possible insufficiency of the treatment approach to childhood BA leading to the symptom takeover through the youth generation, and we should be careful with PH⁺ in non-BA patients who have little BA symptoms. Another valuable finding regarding the effect of PH status is that PH⁻ in possible-BA had decreased airway function compared with PH⁺. This tendency is also observed in current-BA (Table 3). Although the details in the treatment history of BA is limited in the medical record, it is more likely that PH⁺ in these categories received treatment intervention in the past, which may apparently improve the respiratory function, assuming possible-BA has high potential for being true BA.¹⁸

We included questionnaires of respiratory symptoms and PFT at baseline medical check-ups, with the belief that these findings are important in the clinical diagnosis of BA. However, they may be insufficient for the diagnosis of EIB. Rundell, *et al.* found that among elite athletes, a diagnosis based on self-reported symptoms is no more accurate than a coin toss. In that study, 61% of EIB-positive athletes reported symptoms, and 45% of normal pulmonary function athletes reported symptoms of EIB.¹⁹ Methacholine challenge test is often used for BA/EIB diagnosis in Japan, but it should be noted that a relatively low sensitivity for EIB diagnosis especially in summer sports is reported for this provocation.²⁰ We have recently started additional bronchial challenge tests such as eucapnic voluntary hyperpnea and hypertonic saline inhalation, together with exercise challenge which are the current challenge tests also recommended by the International Olympic Committee for the diagnosis of BA/EIB in athletes.

In summary, the PFT results at the Niigata Institute for Health and Sports Medicine were analyzed, according to the historical background of BA, and the prevalence of current-BA, possible-BA, and the cumulative morbidity of BA among the regional elite athletes were 1.1, 6.5, and 8.9%, respectively. A limitation of this study is in the retrospective analysis using a medical questionnaire, of which data had been adopted from sufficient but non-uniform medical record formats. The effectiveness of this medical questionnaire in the uniform medical record format on scoring should be confirmed, and is currently under prospective investigation.

Finally, considering the epidemiological data on BA in athletes available so far, the incidence of BA among the Japanese athletes may be higher than currently recognized. More intervention is encouraged for diagnosing BA and related subtypes to avoid any fatal asthma attacks during sport activities, and to restore originally expected athletic performance of the affected individuals.

ACKNOWLEDGEMENTS

The authors are grateful to Katsutoshi Nishino for expert technical assistance in pulmonary function testing, and to Tetsu Miura for management of the athletic tests.

REFERENCES

1. Fitch KD. Beta2-Agonists at the Olympic Games. *Clin Rev Allergy Immunol* 2006;**31**:259-68.
2. Masoli M, Fabian D, Holt S, Beasley R. The global burden of asthma: executive summary of the GINA Dissemination Committee report. *Allergy* 2004;**59**:469-78.
3. Larsson K, Ohlson P, Larsson L, Malmberg P, Rydstrom PO, Uhrlén H. High prevalence of asthma in cross country skiers. *BMJ* 1993;**307**:1326-9.
4. Weiler JM, Layton T, Hunt M. Asthma in United States Olympic athletes who participated in the 1996 Summer Games. *J Allergy Clin Immunol* 1998;**102**:722-6.
5. Weiler JM, Ryan EJ 3rd. Asthma in United States olympic athletes who participated in the 1998 olympic winter games. *J Allergy Clin Immunol* 2000;**106**:267-71.
6. Chowgule KV, Shetye VM, Parmar JR *et al.* Prevalence of respiratory symptoms, bronchial hyperreactivity, and asthma in a megacity. Results of the European community respiratory health survey in Mumbai (Bombay). *Am J Respir Crit Care Med* 1998;**158**:547-54.
7. Turcotte H, Langdeau JB, Thibault G, Boulet LP. Prevalence of respiratory symptoms in an athlete population. *Respir Med* 2003;**97**:955-63.
8. Hallstrand TS, Curtis JR, Koepsell TD *et al.* Effectiveness of screening examinations to detect unrecognized exercise-induced bronchoconstriction. *J Pediatr* 2002;**141**:343-8.
9. Global Initiative for Asthma. Global Strategy for Asthma Management and Prevention. Available at: <http://www.ginasthma.co./GuidelinesResources.asp?l1=2&l2=0>. Accessed April 30, 2009.
10. Hammerman SI, Becker JM, Rogers J, Quedenfeld TC, D'Alonzo GE Jr. Asthma screening of high school athletes: identifying the undiagnosed and poorly controlled. *Ann Allergy Asthma Immunol* 2002;**88**:380-4.
11. The Ministry of Health, Labour and Welfare of Japan. [Health and welfare survey on allergic symptoms in 2003]. Available at: http://www.dbtk.mhlw.go.jp/toukei/d_ata/230/2003/toukeihyou/0004683/t0099341/Table12_001.html (in Japanese). Accessed January 10, 2009.
12. Becker JM, Rogers J, Rossini G, Mirchandani H, D'Alonzo GE Jr. Asthma deaths during sports: report of a 7-year experience. *J Allergy Clin Immunol* 2004;**113**:264-7.
13. Nicolai T, Illi S, von Mutius E. Effect of dampness at home in childhood on bronchial hyperreactivity in adolescence. *Thorax* 1998;**53**:1035-40.
14. Park ES, Golding J, Carswell F, Stewart-Brown S. Pre-school wheezing and prognosis at 10. *Arch Dis Child* 1986;**61**:642-6.
15. Oswald H, Phelan PD, Lanigan A *et al.* Childhood asthma and lung function in mid-adult life. *Pediatr Pulmonol* 1997;**23**:14-20.
16. Agertoft L, Pedersen S. Effects of long-term treatment with an inhaled corticosteroid on growth and pulmonary function in asthmatic children. *Respir Med* 1994;**88**:373-81.
17. Pedersen S. Can steroids cause asthma to remit? *Am J Respir Crit Care Med* 1996;**153**:S31-2.
18. Kauppinen R, Sintonen H, Vilkkä V, Tukiainen H. Long-term (3-year) economic evaluation of intensive patient education for self-management during the first year in new asthmatics. *Respir Med* 1999;**93**:283-9.
19. Rundell KW, Im J, Mayers LB, Wilber RL, Szmedra L, Schmitz HR. Self-reported symptoms and exercise-induced asthma in the elite athlete. *Med Sci Sports Exerc* 2001;**33**:208-13.
20. Holzer K, Anderson SD, Douglass J. Exercise in elite summer athletes: Challenges for diagnosis. *J Allergy Clin Immunol* 2002;**110**:374-80.

Relationship between radiological knee osteoarthritis and biochemical markers of cartilage and bone degradation (urine CTX-II and NTX-I): the Matsudai Knee Osteoarthritis Survey

Nobuchika Tanishi · Hiroshi Yamagiwa ·
Tadashi Hayami · Hisashi Mera · Yoshio Koga ·
Go Omori · Naoto Endo

Received: 9 September 2008 / Accepted: 6 February 2009 / Published online: 21 April 2009
© The Japanese Society for Bone and Mineral Research and Springer 2009

Abstract Biochemical markers of cartilage and bone degradation are becoming increasingly important in the evaluation of knee osteoarthritis (OA). To clarify the correlation between radiological knee OA and urine CTX-II (C-terminal crosslinking telopeptide of collagen type II) or urine NTX-I (N-terminal crosslinking telopeptide of type I collagen), we conducted a cross-sectional study in the cohorts of the epidemiological knee survey at the Matsudai district in Niigata Prefecture, Japan. Urine specimens were collected from 296 subjects, and CTX-II and NTX-I were measured using ELISA. Standing knee AP X-rays were obtained and graded according to the Kellgren–Lawrence classification. The subjects were then divided by gender, age (40- to 59-year-old group and 60- to 79-year-old

group), and the X-ray grade (Grade 0, 1, Grade 2, and Grade 3, 4). In non-OA (Grade 0, 1) subjects, the 60- to 79-year-old group had significantly higher CTX-II values than the younger group only in females. The subjects of both genders aged over 60 years of age with OA Grade 3, 4 had significantly higher CTX-II values than the Grade 0, 1 group or the Grade 2 group. For NTX-I, there were no significant differences between each OA grade although the Grade 3, 4 group females from 60 to 79 years of age had higher values than the Grade 2 group. In addition, in the 60- to 79-year-old subjects of both genders, a positive correlation was observed between the urine CTX-II and urine NTX-I. For the subjects ranging from 60 to 79 years of age in both genders, the urine CTX-II values indicate the progression of OA. In addition, the weak but positive correlation between urine CTX-II and urine NTX-I in the subjects ranging from 60 to 79 years of age in both genders suggests that bone resorption and cartilage degradation appear to develop in parallel.

N. Tanishi · H. Yamagiwa (✉) · H. Mera · N. Endo
Division of Orthopedic Surgery, Department of Regenerative
and Transplant Medicine, Niigata University Graduate School
of Medical and Dental Sciences, 1-757 Asahimachi-dori,
Chuo-ku, Niigata 951-8510, Japan
e-mail: hymgw@med.niigata-u.ac.jp

N. Tanishi
Department of Orthopedic Surgery, Niigata Rosai Hospital,
Niigata, Japan

T. Hayami
Department of Orthopedic Surgery, Saiseikai Niigata Daini
Hospital, Niigata, Japan

Y. Koga
Department of Orthopedic Surgery, Niigata Kobari Hospital,
Niigata, Japan

G. Omori
Center for Transdisciplinary Research, Niigata University,
Niigata, Japan

Keywords Knee osteoarthritis · Urine CTX-II ·
Urine NTX-I

Introduction

In the last several years, the average age of people in Japan has been increasing rapidly, and knee osteoarthritis (OA) is becoming a very frequently occurring disease. Currently, diagnosis of knee OA is based on symptoms, history, physical findings, laboratory findings of the blood and synovial fluid, image assessments (e.g., X-ray, MRI).

An evaluation of the function and pain in knee OA is performed based on the functional scores (e.g., the Knee Society Score, the Japanese Orthopaedic Association Knee OA score), and QOL assessments (e.g., SF-36, WOMAC

score, Japanese Osteoarthritis Measure score [1]). The findings of each examination and assessment are considered to mainly provide information of the current conditions of knee OA and therefore help to determine the optimal treatment method at that point. However, these findings are insufficient for evaluating the disease activity and predicting the prognosis of knee OA.

Recently, OA biomarkers have been gathering attention as objective indices for early diagnosing knee OA and predicting the degree of progression and prognosis. If useful joint biomarkers are found and can be applied clinically, they would be very beneficial in terms of both medicine and medical economics. Currently, joint biomarkers include substrate markers formed by degradation products of joint tissues such as pyridinoline [2] and cartilage oligomeric matrix protein (COMP) [3], enzymes that exist in the joints such as matrix metalloproteinases (MMPs) [4], tissue inhibitors of metalloproteinases (TIMPs) [5], interleukins [6], other inflammatory cytokines, or nitric oxide (NO) [7]. No definite joint biomarkers, however, have yet been found.

When type II collagen, which is the main component of joint cartilage, is degraded by a cartilage-degrading enzyme, C-terminal crosslinking telopeptide of collagen type II (CTX-II) is produced and excreted through urine. Garnero et al. [8, 9] have reported that the urine CTX-II value was significantly high in patients with early rheumatoid arthritis and that it could be used as an index for reaching diagnosis, thus predicting X-ray progression, and determining the effects of drug therapy. In addition, patients with hip OA exhibited higher values of urine CTX-II than healthy subjects, and cases of rapidly developing hip OA had significantly higher CTX-II values than cases of slowly developing hip OA [10]. Moreover, the urine CTX-II values of patients with developed radiological knee OA were higher [11, 12], thus indicating the possibility that CTX-II can be used joint biomarker that anticipates the progression of knee OA. There have been several reports regarding urine CTX-II, but there are few reports of urine CTX-II being used for Japanese patients with knee OA.

In addition, regarding the correlation between knee OA and osteoporosis, although both conditions are common among females and share similar ages of onset, definite information has not yet been obtained. In recent reports, it has been experimentally revealed that subchondral bone resorption and subsequent bone sclerosis occurs in conjunction with the progression of knee OA [13]. The nature of the changes that occur to bone resorption markers in conjunction with the progression of knee OA is of great interest.

We have conducted a total of four epidemiological surveys on knee OA at intervals of 7 years during the 21 years from 1979 to 2000 in Matsudai district (formerly

Matsudai-machi) in Tokamachi, Niigata Prefecture, Japan during which time resident health checks were conducted every year, and we have published a number of reports regarding the risk factors of knee OA [14, 15]. To provide the first step in verifying our hypothesis that urine CTX-II can be used as a joint biomarker for knee OA, we investigated the correlation between the knee OA X-ray grades obtained from the same cohorts and the urine CTX-II values as well as the urine NTX-I (N-terminal crosslinking telopeptide of type I collagen) values, which is a bone metabolism biomarker, while taking the age and gender of the subjects into consideration.

Subjects and methods

For the resident annual health check-up conducted in the Matsudai district in Tokamachi City, Niigata Prefecture in 2006, we mailed a letter requesting the cooperation of the residents who had been randomly selected in advance based on their resident registration code numbers, and we then collected urine specimens and took standing AP X-rays of their knees for 296 subjects from whom consent was obtained on the day of the health check. The study protocol was approved by the Ethical Committee of Niigata University Graduate School of Medical and Dental Sciences.

Blind X-ray assessments were conducted by the two senior authors (G. O. and Y. K.), in accordance with the Kellgren–Lawrence classification, and whenever there was a difference in grade between right and left, the higher grade was employed. As with the past reports, the grades 0 and 1 were defined as the non-OA group and grades 2 or more were defined as the OA group. Table 1 shows the X-ray grades of the knee OA of the cases, the number of the subjects, and their age distribution.

The urine specimens were stored at -80°C after being collected, CTX-II was measured using a Urine CartiLaps enzyme linked immunosorbent assay (ELISA) kit (Nordic

Table 1 Demographics of subject's age, gender, and X-ray grade of knee OA

Number of subjects	X-ray grade of knee OA			
	G 0, 1	G 2	G 3	G 4
Total	106	126	45	19
Age (years) ^a	60 ± 14.7	67.3 ± 9.3	73.1 ± 6.6	75.8 ± 5.6
Male	47	55	17	6
Age*	61.6 ± 15.5	69.4 ± 9.3	76.9 ± 6.0	74.7 ± 3.1
Female	59	71	28	13
Age	58.7 ± 14.0	65.7 ± 9.1	70.9 ± 6.0	76.4 ± 6.5

^a Mean ± SD